Journal of Drug Delivery Science and Technology 57 (2020) 101584

Contents lists available at ScienceDirect

Journal of Drug Delivery Science and Technology

journal homepage: www.elsevier.com/locate/jddst

Preparation and *in-vitro* evaluation of pH-responsive cationic cyclodextrin coated magnetic nanoparticles for delivery of methotrexate to the Saos-2 bone cancer cells

Delshad Ahmadi[a,b], Mojtaba Zarei[a], Mahdi Rahimi[c], Marzieh Khazaie[a], Zatollah Asemi[d], Seyed Mostafa Mir[b,e], Alireza Sadeghpour[f], Ansar Karimian[a], Fourogh Alemi[a,g], Mohammad Rahmati-Yamchi[b], Roya Salehi[h], Farhad Jadidi-Niaragh[i], Mehdi Yousefi[i], Nafiseh Khelgati[a], Maryam Majidinia[j,**], Amin Safa[k,***], Bahman Yousefi[a,b,l,*]

[a] *Drug Applied Research Center, Tabriz University of Medical Sciences, Tabriz, Iran*
[b] *Department of Biochemistry and Clinical Laboratories, Faculty of Medicine, Tabriz University of Medical Sciences, Tabriz, Iran*
[c] *Institute of Polymer and Dye Technology, Lodz University of Technology, Stefanowskiego 12/16, 90 924, Lodz, Poland*
[d] *Research Center for Biochemistry and Nutrition in Metabolic Diseases, Kashan University of Medical Sciences, Kashan, Iran*
[e] *Students Research Committee, Babol University of Medical Sciences, Babol, Iran*
[f] *Department of Orthopedic Surgery, Faculty of Medicine, Tabriz University of Medical Sciences, Tabriz, Iran*
[g] *Students Research Committee, Tabriz University of Medical Sciences, Tabriz, Iran*
[h] *Department of Medical Nanotechnology, Faculty of Advanced Medical Sciences, Tabriz University of Medical Sciences, Tabriz, Iran*
[i] *Immunology Research Center, Tabriz University of Medical Sciences, Tabriz, Iran*
[j] *Solid Tumor Research Center, Urmia University of Medical Sciences, Urmia, Iran*
[k] *Institute of Research and Development, Duy Tan University, Da Nang, Viet Nam*
[l] *Molecular Medicine Research Center, Tabriz University of Medical Sciences, Tabriz, Iran*

ARTICLE INFO

Keywords:
Cationic nanoparticles
Drug delivery systems
Osteosarcoma
And methotrexate

ABSTRACT

Osteosarcoma, as a common malignant neoplasm in children and adolescents, still remains a challenge for conventional therapeutic regimens. In the meantime advent of innovative and revolutionary techniques such as drug delivery systems and smart nano-biomaterials seems promising in tackling these complications. In this study, we designed a smart nano-system consisting of a magnetic inner core and polymeric outer shell with cationic moieties for targeted delivery and enhanced uptake of methotrexate anticancer agent for Saos-2 cell line. The designed nano-formulation was characterized and its drug loading capacity and drug release profile were studied as well that about 60% of methotrexate was released in the first 12 h. The efficacy of the nano-formulation in killing cancer cells was assessed using MTT, cellular uptake, and uptake flow-cytometry. Our *in-vitro* results confirmed the prepared nano-system has a potential for delivery of anticancer drugs against the Saos-2 cell line and suggests more investigations such as *in-vivo* tests to be implemented.

1. Introduction

Osteosarcoma is one of the most common cancers in children and adolescents [1]. About 70% of cases occur in people between 10 and 20 years of age [2]. It is the deadliest form of bone malignancy [3] and this kind of cancer tumor commonly appears at end parts of long bones such as femur, tibia, and humerus (near the metaphyseal growth plates) [4].

A combination of surgery, chemotherapy, and radiotherapy makes up the common treatment regimen for this cancer [5,6]. Among chemotherapy agents like ifosfamide, doxorubicin, etoposide and methotrexate the latter is one of the highest prescribed anticancer drugs in the world, hence it has now been the subject of interest among researchers for its tunable pharmacokinetic parameters [7,8]. Methotrexate (MTX) is an antimetabolite agent, killing cancer cells by disrupting the folate metabolism pathway [9]. As a widely used drug in the treatment of various malignancies, methotrexate has gained a reputation among

* Corresponding author. Drug Applied Research Center, Tabriz University of Medical Sciences, Tabriz, Iran.
** Corresponding author.
*** Corresponding author.
E-mail address: yousefib@tbzmed.ac.ir (B. Yousefi).

https://doi.org/10.1016/j.jddst.2020.101584
Received 26 November 2019; Received in revised form 11 February 2020; Accepted 12 February 2020
Available online 29 February 2020
1773-2247/

many other anticancer medications and even proved to be an effective anti-inflammatory and an effective treatment for arthritis though its unfavorable side effects still remain to be a concern [10,11].

In the meantime, progresses in drug delivery systems such as developments of effective nanocarriers seem effective in reducing drug side effects, increasing its bioavailability in tumor site and eventually reducing the total amount of the required drug dosage [12,13]. Poor water solubility, low plasma half-life, and low permeability are prominent negative features of MTX that easily can be addressed by loading it into a proper carrier [14].

During recent years vast numbers of nanoparticle-based delivery systems had been developed for delivery of anticancer drugs [15,16]. Among these, polymeric based carriers such as liposomes, dendrimers, and magnetic nanoparticles are preferable for general favorable characteristics like the ease of preparation; single-step drug loading method, constituent's availability and cost efficiency [17–20].

In recent years cationic drug carrier is gaining attention within the research communities for their favorable features such as their fast and large uptake, less cytotoxicity and important of all their non-edocytotic entry into cells [18,21]. Therefore, cationic polymer-based nanocarriers are desirable in the delivery of anionic drugs such as MTX due to electrostatic interaction between carriers and loaded drugs in physiological conditions. The ionic interaction between the drug and its carrier and the dependence of this interaction on the pH of the media makes it a desirable candidate for pH-sensitive delivery systems.

Herein, we developed a synthetic polymer with cationic moieties on the surface of magnetic nanoparticles with cyclodextrin anchoring sections to deliver MTX as a chemotherapeutic agent to the Saos-2 bone cancer cells. The prepared nano-platform was characterized and validated by several techniques such as FTIR, SEM, EDS, XRD, DLS, and zeta potential. The biocompatibility of the platform was evaluated by hemolysis assay on human red blood cells. Further *in-vitro* studies were carried out on Saos-2 cell lines, and the rate of increase in drug efficacy confirmed by the use of nano-platform with biological assays, including uptake assay, flow cytometry, and MTT assay.

2. Materials and methods

2.1. Materials and reagents

β-Cyclodextrin (β-CD, 98%), p-toluenesulfonyl chloride (TsCl, 99%), and imidazole (Imz, 99%) were purchased from Sigma-Aldrich Co. 2,2′-Azobis(2-methylpropionitrile) (AIBN, 98%), ammonia solution (28%), ferric chloride hexahydrate ($FeCl_3.6H_2O$), ferrous chloride tetrahydrate ($FeCl_2.4H_2O$), allyl imidazole, dimethylformamide (DMF), dimethylsulfoxide (DMSO), other solvents and all other chemical reagents were provided from Merck Co and used as received. Roswell Park Memorial Institute 1640 growth medium (RPMI), trypsin, and fetal bovine serum (FBS) obtained from Gibco BRL Life Technologies. Methotrexate was purchased from Zahravi Pharmaceutical Co. (Tabriz, Iran) and 3-(4, 5- dimethylthiazol-2-yl)-2, 5-diphe-nyltetrazolium bromide (MTT) was provided from Bio Basic Inc. (Markham, Canada). Human red blood cells (HRBCs) were obtained from the Iranian Blood Transfusion Institute and become stable with ethylenediamine tetra acetic acid (EDTA).

Synthesis of quaternized ammonium alkyl halide N,*N*-dimethylaminoethyl methacrylate (QDMAEMA) and 3-(trimethoxysilyl)propyl methacrylate (TMSMA) as monomers according to the recent articles and used in this study [22,23]. Mono substituted tosylated β-cyclodextrin (Ts-CD) was synthesized according to a reported method [24].

2.2. Instrumentation

Chemical structures of samples were done with Fourier transform infrared (FTIR) spectroscopy in the range of 500–4000 cm^{-1} by Bruker Tensor 270 spectrometer. The morphology, size, and elemental percentage analysis of samples were examined using a Field Emission Scanning Electron Microscopy and Energy Dispersive X-ray (FESEM-EDX; S4160 Hitachi, Japan). Samples were attached to a metal stub using a carbon double-sided adhesive tape and enclosed with a thin layer of gold, by using a direct current sputter technique (Emitechk450X, England). Atomic and molecular structure of a crystal was examined with X-ray Rigaku Utma 4 diffractometer, power of 50 kV/50 mA and Cu Ka irradiation, in an angle range (2θ) of 10–80°, at room temperature. XRD was done X' Pert Pro, Malvern Panalytical Ltd (Almelo, Netherlands). The measurements of average diameter and zeta-potential of nanoparticles, laser-scattering techniques were performed at 25 ºC by Zetasizer Nano ZS90; Malvern Instruments, Malvern, UK.

2.3. Preparation of cationic magnetic nanocarrier (Cat-MN)

a Preparation allyl imidazole grafted CD (Aly-Imz/CD)

2.0 g of Ts-CD was dissolved in 40 ml DMF and 6.65 g of allyl imidazole was then added to the solution under magnetic stirring at 90 °C for 24h. After completion of the reaction and cooling to room temperature, the reaction solution was precipitated in the excess amount of acetone. Then, DMF was removed by a rotary evaporator and washed with acetone several times to obtain allyl imidazole grafted β-CD (Aly-Imz/CD) [25].

b Synthesis of cationic nano-platform as a magnetic nanocarrier (Cat-MN)

In a common free radical polymerization reaction, Aly-Imz/CD (0.3 g) was added to a mixture of QDMAEMA (0.3 g) and TMSMA-MNPs (0.4 g) in DMSO under nitrogen atmosphere. Then AIBN catalyst (5 mg) was added and the reaction was allowed to complete under stirring at 80 °C for 2 days. The final product was precipitated in cold acetone and was collected by centrifugation (5000 rpm, 5 min). Finally, cationic magnetic nanocarrier (Cat-MN) was dried by freezing dry method and utilize as a nano-platform.

2.4. MTX loading

For MTX loading on the nano-platform, 8 mg of Cat-MN was dispersed in 80 mg mL^{-1} MTX solution and stirred at room temperature in a sealed vial at the dark condition for 24 h. Then, the supernatant was separated out by an external magnetic field and its optical density was measured by UV-VIS spectroscopy at 290 nm.

In order to determine the concentration of MTX loaded into nano-platform, the calibration curve for varying concentrations of free MTX was drawn based on unloaded drug concentration on the supernatant. Drug loading efficiency (DLE) and drug encapsulation efficiency (DEE) of MTX were calculated by the following formulas:

$$\text{Drug Loading efficiency}\left(\%\ \frac{w}{w}\right) = \frac{\text{Mass of MTX in the Cat} - \text{MN}}{\text{Mass of the Cat} - \text{MN}} \times 100$$

$$\text{Drug encapsulation efficiency}\left(\%\ \frac{w}{w}\right) = \frac{\text{Mass of MTX in the Cat} - \text{MN}}{\text{Mass of MTX}} \times 100$$

The resultant precipitate (MTX/Cat-MN) was washed with an adequate amount of PBS and vacuum-dried for further *in-vitro* studies.

2.5. In-vitro release of MTX from the nano-platform

MTX release assessment from nano-platform was carried out in various pH solutions 5.0 and 7.4 of the simulated cancer tissue microenvironment and physiological condition, respectively. For this purpose, 10 mg of MTX/Cat-MN were dispersed in 1 mL PBS buffer with

two pH values and were shaken in the incubator at 37 °C. Then, the supernatant was collected using an external magnetic field within a prearranged time steps (1h, 2h, 4h, 6h, 12h, 24h, 48h, 72h, and etc.) and the supernatants' absorbances were measured at 290 nm via a UV–vis spectrophotometer.

The calibration curve of MTX was used as a criterion for converting the released MTX absorbance to its concentration. Lastly, the drug release amount at any given time was calculated the following formula.

$$\text{Drug release (\%)} = \frac{ammount\ of\ MTX\ release\ in\ medium}{amount\ of\ MTX\ loaded\ in\ the\ nano-platform} \times 100$$

2.6. Hemolysis assay

Hemolysis assay was carried out for biocompatibility assessment of synthesized nano-formulation [17]. For this analysis, 1 mL of EDTA stabilized human red blood cells (RBCs) were washed three times with PBS until getting a clear supernatant (centrifugation at 2500 for 10 min) and then pellets (RBCs) were diluted with deionized water. Then, 0.5 mL of the RBCs suspensions were incubated with 0.5 mL of different concentration of Cat-MN (with final concentrations: 1280, 640, 320, 160, 80, 40, 20 and 10 μg mL^{-1}). Also, 0.5 mL of RBCs suspensions were incubated with 0.5 mL of deionized water and PBS solution as positive (100% hemolysis rate) and negative control (0% hemolysis rate), respectively. All samples were shaken at 37 °C for 4 h and centrifuged at 1000 rpm for 15 min. At last, 200 μL of supernatant was transferred to a 96-well plate, and the absorbance value at 540 nm was measured using an ELISA reader. The hemolysis rate was measured using the following formula:

$$\text{Hemolysis (\%)} = \frac{OD_{sample} - OD_{negative.c}}{OD_{Positive.c} - OD_{negative.c}} \times 100$$

2.7. Cellular uptake assay

The flow cytometry and fluorescence microscopy were utilized for intracellular uptake measurement Cat-MN into cells. Due to the non-fluorescent properties of MTX, MTX/Cat-MN was labeled with rhodamine-B (rho-MTX/Cat-MN) as a marker to track its cellular uptake process [26].

Uptake measurement with fluorescence microscopy: in order to observe rho-MTX/Cat-MN uptake within cells, after seeding approximately 20 × 10^3 Saos-2 cells in slide champers well and incubation for 24 h, the cells were treated with free rho-MTX/Cat-MN at IC_{50} concentration. Then the cells were washed with PBS buffer after 1 and 2 h and observed with fluorescent microscopy (Olympus microscope Bh2-RFCA, japan).

Uptake measurement with flow-cytometry: The Saos-2 cells (500 × 10^3 cells per well) were seeded in the six-well plate and incubated for 24 h. After treatment for 1 and 2 h with rho-MTX/Cat-MN at a concentration of IC_{50}, the cells were washed with PBS and observed with FACScalibur flow-cytometer to determine the fluorescent intensity related to rhodamine-labeled Cat-MN uptake within the cells. The non-treated cells were considered as a negative control.

2.8. Cell culture and in-vitro cytotoxicity assay

Sarcoma osteogenic cells (Saos-2) were cultured in RPMI (containing penicillin-streptomycin) with 10% FBS and incubated for 48 h in 37 °C [27]. The *in-vitro* cytotoxicity of nanocarrier, free MTX, and MTX/Cat-MN was performed against the Saos-2 cells using the MTT assay. For this purpose, 15,000 cells were seeded in each well of a 96-well plate. Adequate quantity of growth medium with 10% fetal bovine serum (FBS) was added to bring the volume of each well to 200 λ, then the plate incubated at 37 °C in a humidified atmosphere with 5% CO_2 for 24 h to allow cells to properly attach to the bottom of the wells. Then, the cells were treated with the closed up the concentration to IC_{50} according to other literature (serial dilution of free MTX, free Cat-MN and MTX/Cat-MN). Also, for each of these groups, a corresponding non-treated control group was assigned. The microplate solutions were removed after incubation for 48 h and wells were washed with PBS. 20 λ MTT reagent and 180 λ of growth medium with 10% FBS was added to each well. After the incubation for an additional 4 h, the medium containing unreacted MTT reagent was removed carefully from each well. Then formazan crystals were dissolved with the addition of 150 μl of DMSO to each well. The solubilized formazans' absorbance at 570 nm was determined by the ELISA plate reader and growth inhibition was calculated. All tests were done in triplicate. The cell viability percentages were calculated via the following formula:

$$\text{Cell viability (\%)} = \frac{\text{The absorbance of each test}}{\text{Mean absorbance of controls}} \times 100$$

3. Results and discussion

3.1. Preparation of cationic magnetic nanocarrier (Cat-MN)

In the present study, the pH-responsive Cat-MN as a magnetic nano-

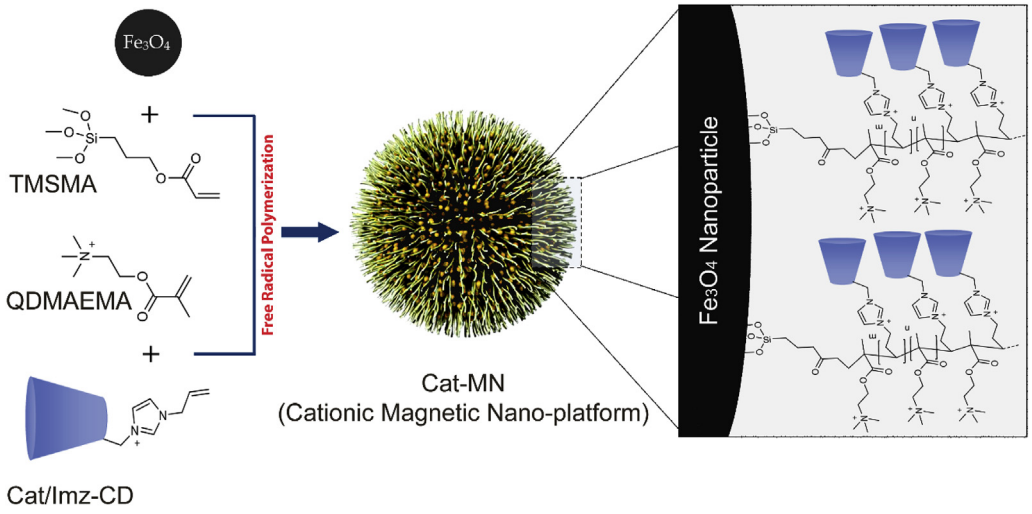

Fig. 1. Preparation process and proposed branch structure of Cat-MN as a cationic magnetic nano-platform for delivery of MTX anticancer drug.

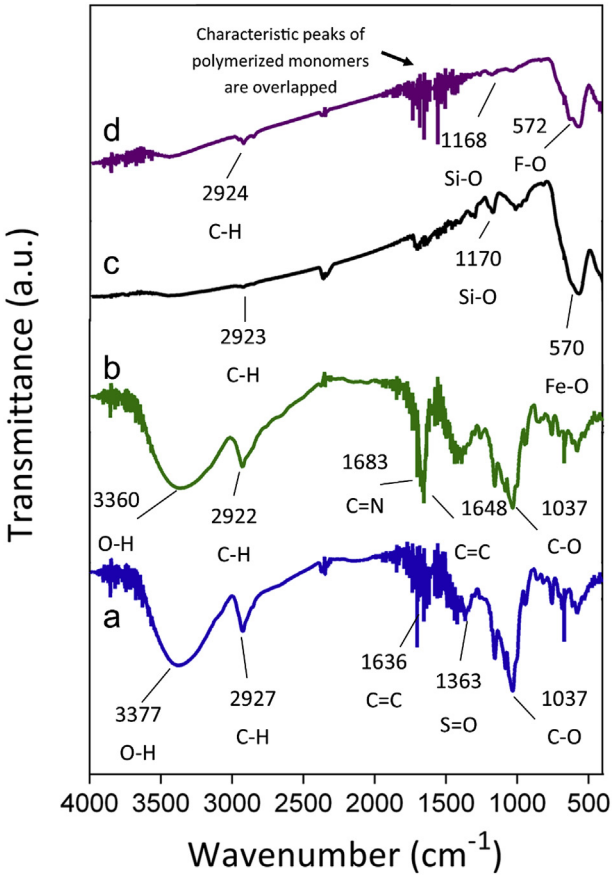

Fig. 2. FTIR spectra of Ts-CD (a), Aly-Imz/CD (b), TMSMA-MNPs (c), and Cat-MN (d).

system was prepared in facile steps as illustrated in Fig. 1. Firstly, a quaternized cyclodextrin with allyl imidazole moiety was synthesized and polymerized on the surface of acrylate and quartered ammonium functionalized magnetic nanoparticles to form a branched like particles. Due to the presence of cationic sites on the polymeric chains, it was expected that this platform could be acted as a delivery system of anionic drugs. Therefore, MTX as a model anticancer drug was loaded on the Cat-MN to determine the ability of nano-system in delivery of MTX to Saos-2 cancer cells. After characterization and MTX loading steps, the biocompatibility and cellular cytotoxicity of nanocarrier was also investigated by several biological assays.

3.2. Characterizations

After preparation of characterizations including FTIR, XRD, SEM, EDX, DLS, and zeta potential. All characterizations were discussed separately as well.

The chemical structure and functional group of each synthesized sample were evaluated by FTIR spectroscopy. Fig. 2 shows the FTIR spectra of Ts-CD (a), Aly-Imz/CD (b), TMSMA-MNPs (c), and Cat-MN (d). The FTIR spectrum of Ts-CD showed a broad peak at around 3377 cm^{-1} and attributed to the hydroxyl groups (-OH). The C–H aliphatic characteristic peak appeared at 2927 cm^{-1} around and C–O has a relatively strong peak at 1037 cm^{-1}. Another characteristic C=C and S=O peaks were appeared at 1636 and 1363 cm^{-1} with strong intensity, respectively. The Aly-Imz/CD has shown two different peaks at 1648 and 1683 cm^{-1} corresponding to the C=C and C=N bonds with strong intensities. After polymerization reaction on the surface of TMSMA-MNPs, two absorbance bonds related to the Si–O and Fe–O are also observed at 572 and 1168 cm^{-1}, respectively. However, the characteristic peaks of polymerized monomers are overlapped and

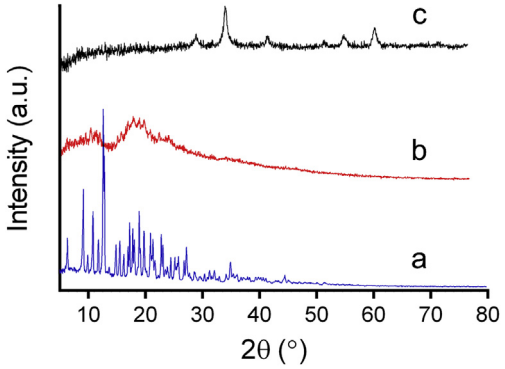

Fig. 3. XRD diffraction of β-CD (a), Aly-Imz/CD (b), and Cat-MN (c) at 2θ range of 5–80°.

could not be observed and distinguished well.

The crystalline structure of β-CD (a), Aly-Imz/CD (b), and Cat-MN (c) were evaluated by XRD analysis (Fig. 3). A series of sharp and intense diffraction peaks have appeared for β-CD revealing crystalline characteristics at wavenumber (2θ) around 6.34, 9.87, 10.79, 12.80 13.63, 16.93, 18.03, 18.62, and 19.09°. Whereas, the XRD analysis of Aly-Imz/CD showed a completely different crystalline structure with smooth and broad peaks around 2θ ~11° and 19° and all sharp and intense peaks were disappeared for Aly-Imz/CD. The characteristic peaks for Cat-MN are at 2θ = 30.30°, 35.66°, 43.34°, 53.74°, 57.33°, and 62.92°. The Debye–Scherrer formula ($D = K\lambda/(\beta \cos\theta)$) was also used to determine the size of Cat-MN. The characters including D, K, λ, and β are in order particle size, constant number (equal to 0.9 for Cu-Ka), the X-ray wavelength (0.15405 nm for Cu-Ka), and the peak width at half-maximum and θ is the diffraction angle (Bragg angle). After calculation, the size of Cat-MN was obtained around 12.55 nm.

SEM produces images of samples by scanning the surface with a focused beam of electrons. The surface morphology of β-CD (a), Aly-Imz/CD (b), and Cat-MN (c) evaluated by SEM analysis (Fig. 4). The results showed that the morphology of β-CD is relatively smooth with a slight wrinkle. These wrinkles cause crystalline with intense peaks in the XRD diffraction. After surface modification of β-CD to produce Aly-Imz/CD, no significant morphology changes were seen, only the amount of wrinkle was reduced. At last, polymerization of synthesized Aly-Imz/CD monomer with QDMAEMA on the TMSMA-MNPs formed a spherical nano-sized particle (Cat-MN) with the size range of 20–80 nm (see Fig. 5).

By using Energy-dispersive X-ray spectroscopy estimate the percentage of different elements in β-CD (a), Aly-Imz/CD (b), and Cat-MN (c). The results showed that β-CD consists of two main elements of C and O, with a weight percentage of 87.9% and 12.1%. After surface modifying of β-CD to form Aly-Imz/CD monomer, the atomic percentage of C and O changed to 53.1% and 29.5%, respectively, and the new peak was observed for N with 17.5%. The N atom refers to the imidazolium quaternized moiety. Finally, the decorating magnetic nanoparticles with polymerization reaction on the TMSMA-MNPs causes changed the percentage of elements to 25.4%, 21.7%, 5.3%, and 47.6% for C, O, N and Fe, respectively.

Various factors such as sample concentration and type of media could alter the hydrodynamic size of particles in the aqueous media which can be measured via DLS technique. The appropriate size for a nano-sized drug carrier is lower than 100 nm to gain an internalization capability into the cells. The suspended bare Fe_3O_4 and Cat-MN have monodispersed peaks with the particle size distribution of about 861.4 ± 68.8 nm and 687.8 ± 17.4 nm, respectively. The obtained results are completely different from SEM and XRD analysis because this technique showed the hydrodynamic size. In contrast, SEM shows the size of the nanoparticles in the dried form.

The surface charge of bare Fe_3O_4 was altered after surface

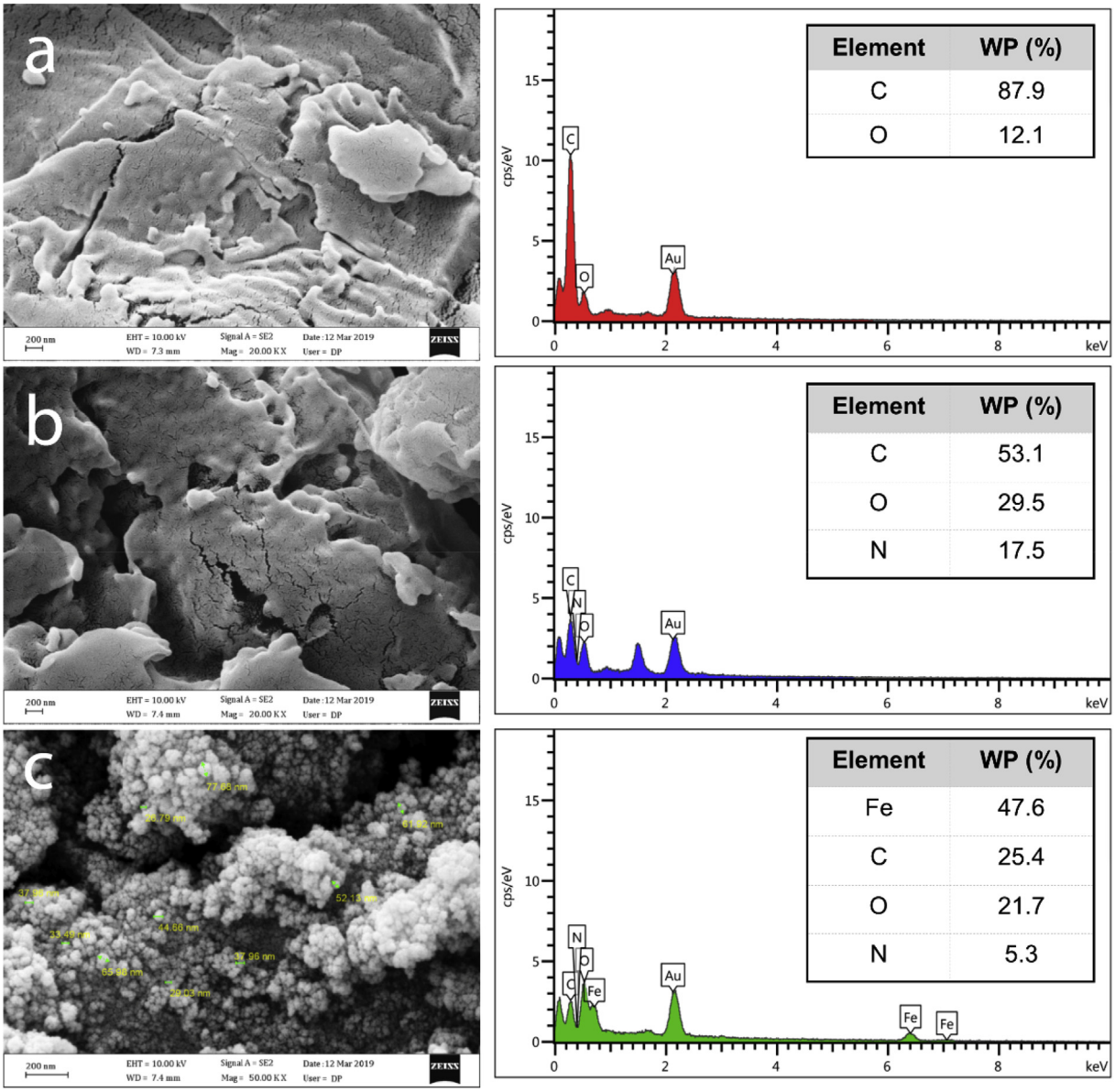

Fig. 4. SEM and EDX analysis with weight percentages (WP %) of elements (carbon, oxygen, nitrogen, and iron) of β-CD (a), Aly-Imz/CD (b), and Cat-MN (c).

modification with cationic polymer and decreased the surface charge from −14.2 mV to −9.3 mV. This result confirmed that the cationic polymer could reduce the inherent negatively charge of Fe_3O_4 magnetic nanoparticles.

3.3. In-vitro DOX loading and release study

MTX, a hydrophobic anticancer drug with carboxylic acid functional groups was used to evaluate loading and controlled drug release natures of MTX as well as the ability for adsorption by prepared Cat-MN as a targeted drug delivery system. There is a permanently positive charge (imidazolium and ammonium sections; Fig. 1) on the surface of Cat-MN which helps to the drug loading. MTX (pKa 4.6 and 5.6) has carboxylic acid functional with an anionic form at pH 7.4. Hence, at this pH, MTX loading can occur via ionic interaction between carboxylate anions exiting in the structure of MTX and functional groups on the surface of the nanocarrier. In addition, the interior hydrophobic cone of CDs presents the ability for enhancing the encapsulation efficiency of MTX. Therefore, these methods can enhance the loading capacity of the nanosystem. The unloaded drug was collected in order to estimate loading efficiency and encapsulation efficiency. The DLE and DEE were obtained at 8.92% and 89.27% respectively. The cumulative MTX release from the nanocarrier under different pH values (physiological condition pH 7.4 and tumoral tissue condition pH 5.0) were tested in order to determine whether the pH value can impress MTX releasing behaviors. All results are illustrated in Fig. 6. At pH 7.4 about 44.21 ± 2.98% of MTX was released from the MTX/Cat-MN after about 300 h, whereas under acidic conditions (pH 5.0), up to 72.73 ± 3.19% of total encapsulation drug was released.

By reducing the pH value of the environment to the pKa value of MTX (4.8 and 5.6) or below it, the carboxylate anion of MTX was protonated. This causes the impairment of the electrostatic interactions between MTX and the Cat-MN protonated functional groups. Hence this can be responsible for accelerating drug release. The second pKa of MTX (4.8) can cause some of deprotonated MTX that remain interacted with the Cat-MN and might be related to the uncompleted release of MTX. According to the above results, it can be claimed that the nanoplatform has a good pH-sensitive nature.

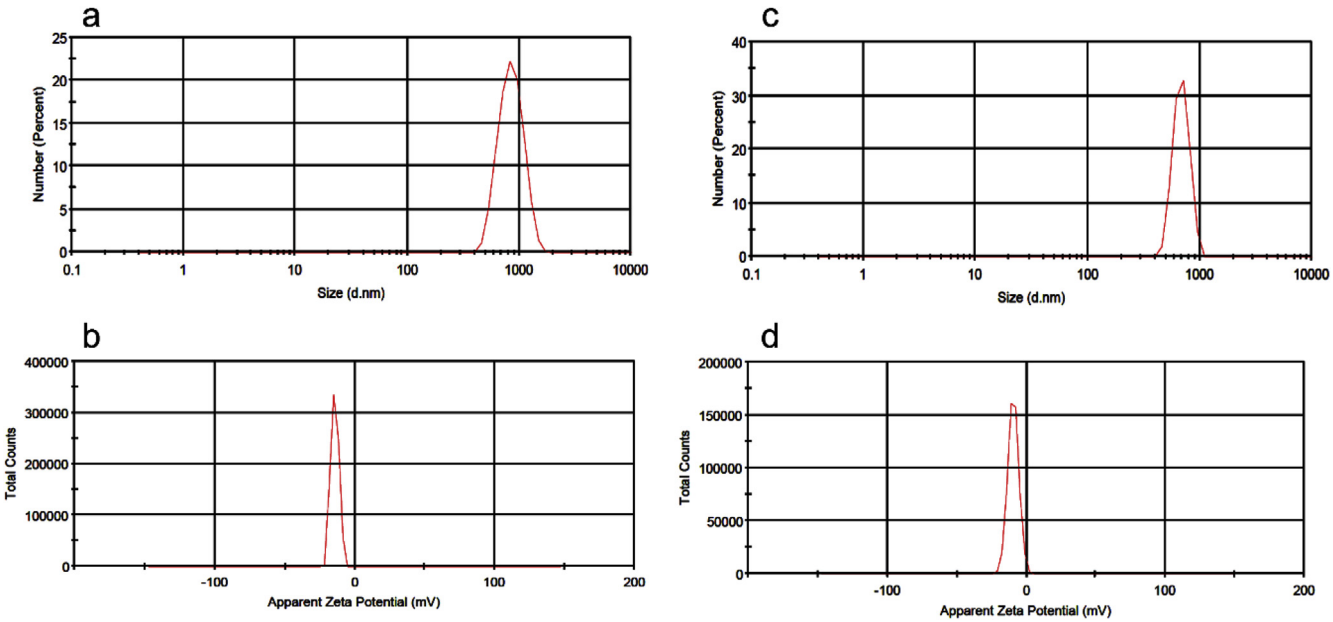

Fig. 5. DLS and zeta potential analysis of Fe_3O_4 (a–b) and Cat-MN (c–d).

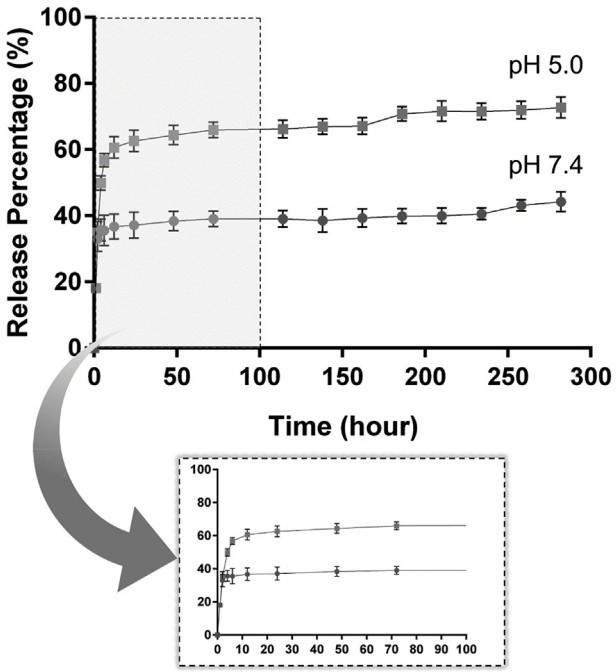

Fig. 6. MTX release profile under both physiological and acidic tissue conditions at 37 °C.

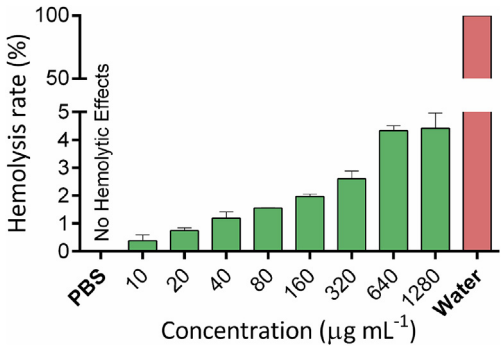

Fig. 7. Hemolysis assay: hemolytic effects of different concentrations of Cat-MN on HRBS after treatment at 37 °C for 4 h (negative control: PBS, positive control: water).

3.4. Hemo-compatibility evaluation

Hemolysis assay which simply is based on the susceptibility of human RBCs membrane to toxic materials were carried out. In this regard, RBCs were exposed to eight different concentrations of Cat-MN (10–1280 μg mL^{-1}) and after centrifugation, the supernatant was taken out and its optical density was measured at 540 nm using UV–vis spectroscopy. As can be seen in Fig. 7 under physiological condition even at higher doses of nanocarrier, its hemolytic effect on RBCs membrane was evaluated as insignificant Also, the results were compared with negative (PBS) and positive (deionized water) control with the hemolysis rate of 0% and 100%, respectively. Our results confirmed the Cat-MN is a hemocompatible nano-system and a suitable candidate for drug delivery and blood-contacting applications (see Fig. 8).

3.5. In-vitro cytotoxicity assay by MTT assay

In-vitro cytotoxicity of the free MTX, MTX/Cat-MN and blank Cat-MN were evaluated by MTT assay for 48 h (Fig. 7). Toxicity assessment of Cat-MN on the Saos-2 cell line showed that even in high concentration (400 μg mL^{-1}) is not toxic and cells survived absolutely (IC_{50} ~ no reached). Therefore our results indicated that the designed nano-platform is safe and biocompatible for drug delivery applications.

To compare the survival rate of Saos-2 cell when exposed to free MTX, MTX/Cat-MN and blank Cat-MN, cells were treated with varying concentrations of mentioned substances and toxicity of each one was evaluated. The IC_{50} value for free MTX after 48 h was reported 7.82 μg mL^{-1} and the IC_{50} value of MTX/Cat-MN after 48 h was reported 7.22 μg mL^{-1}. From the obtained results it can be said that cytotoxic effects of MTX/Cat-MN on Saos-2 cells increased and IC_{50} was reduced. Our results also indicated that cytotoxicity of MTX/Cat-MN and free MTX is a dose-dependent process and IC_{50} rate decreases over the increasing the treating dose.

3.6. Cellular uptake assay

In order to determine the amount of rho/Cat-MN internalization

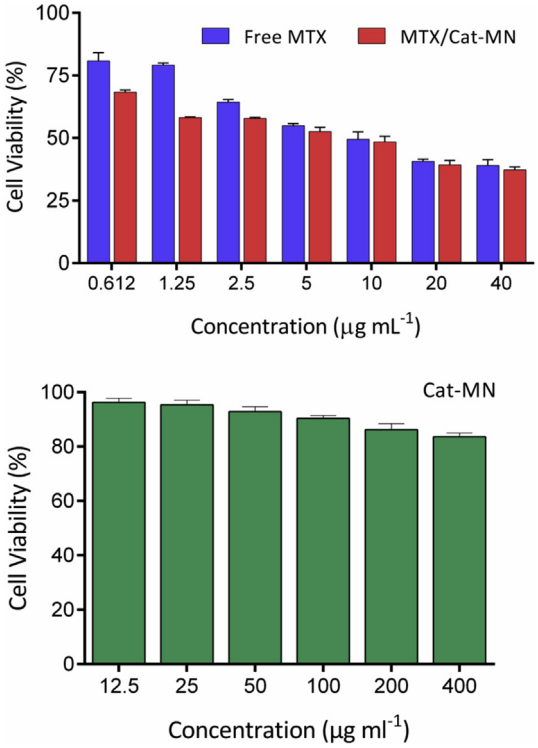

Fig. 8. Cell growth inhibition rate by different concentration of free MTX, MTX/Cat-MN and Cat-MN for 48 h treatment.

into the Saos-2 cells, fluorescence microscopy imaging as a qualitative evaluation was carried out (Fig. 9). The internalization rate by Saos-2 cells indicated that a significant amount of rho/Cat-MN was taken up rapidly by the Saos-2 cells during the first hour of treatment. The results confirmed that the uptake process is completed at the first 1 h. To compare the intensity of fluorescence, the cells were also treated with free rhodamine (Fig. 9A). Quantitative evaluation of the uptake process was performed by flow cytometry cell analysis technique at 1 and 2 h. As can be seen, 99.21% of the MTX/Cat-MN was taken up by the Saos-2 cells after 1st hours (Fig. 9B).

Cationic nano-platform due to their positive net surface charge is capable of strong cellular interaction and intense cell uptake. Another reason for the higher efficacy of this nano-system in comparison to their conventional counterparts is their - non-endosomal cell entry. Within this mechanism, they effectively evade endo/lysosome entrapment of internalized particles and transport cargo (drugs) efficiently into the cytoplasm where it will make its effect on the DHFR enzyme (Fig. 10).

In contrast to sustained release drug delivery systems that are suitable for chronic diseases such as Asthma, Diabetes, and Arthritis, sustained release of the therapeutic agent in cancer could easily cause drug resistance by mechanisms such as ABC-transporters. In the case of cancer explosive and fast release of therapeutics are more suitable for killing cells and preventing them from developing resistance thus cationic nanoparticles with non-endocytic uptake pathway seems promising carriers for delivery of anticancer agents.

4. Conclusion

The most important properties of an ideal carrier are such as stability, nano-size shaped, high drug loading, and biocompatibility with no cytotoxic effects. In this regard, a cationic magnetic drug carrier was developed and used in the treatment of Saos-2 cells line (sarcoma osteogenic cells). Physicochemical characterizations validated our platform synthesize and loading MTX on the platform was done with high loading and encapsulation efficiencies (8.92% and 89.27%). The *in-vitro* release profile showed that the Cat-MN as a cationic magnetic nano-system has pH-responsive property. The biocompatibility evaluation of prepared drug carrier was proved by MTT and hemolysis assays, and

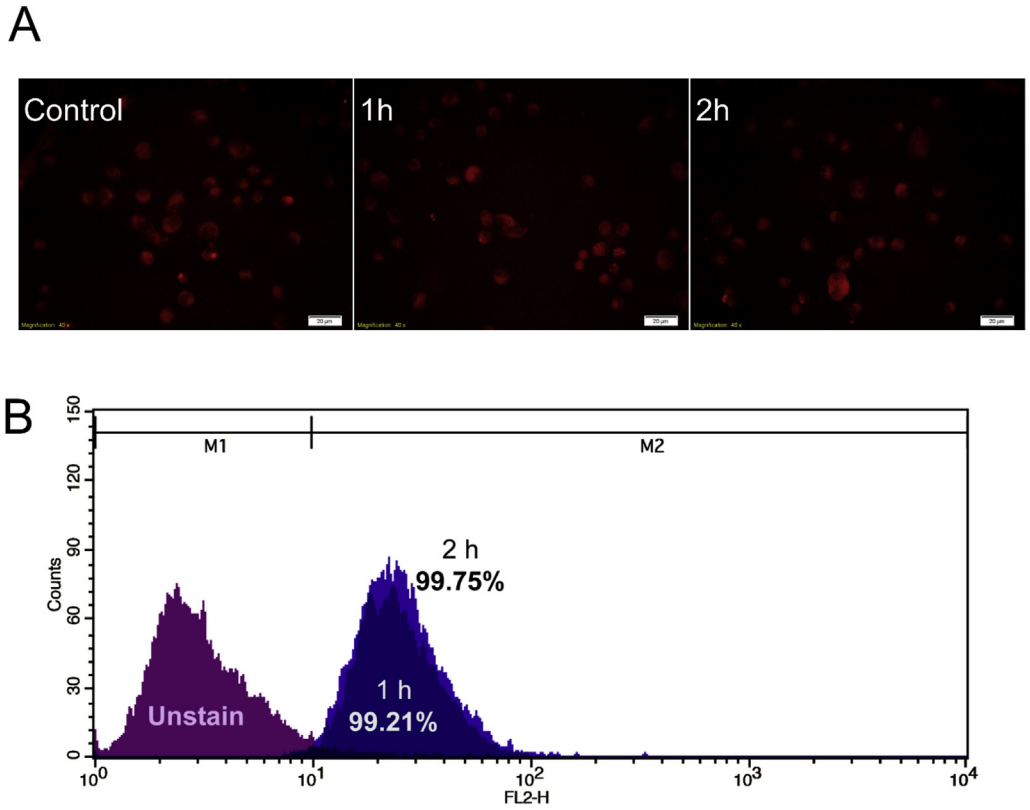

Fig. 9. Cellular uptake percentage of rho-MTX/Cat-MN by Saos-2 cells for treatment for 1.0 and 2.0 h.

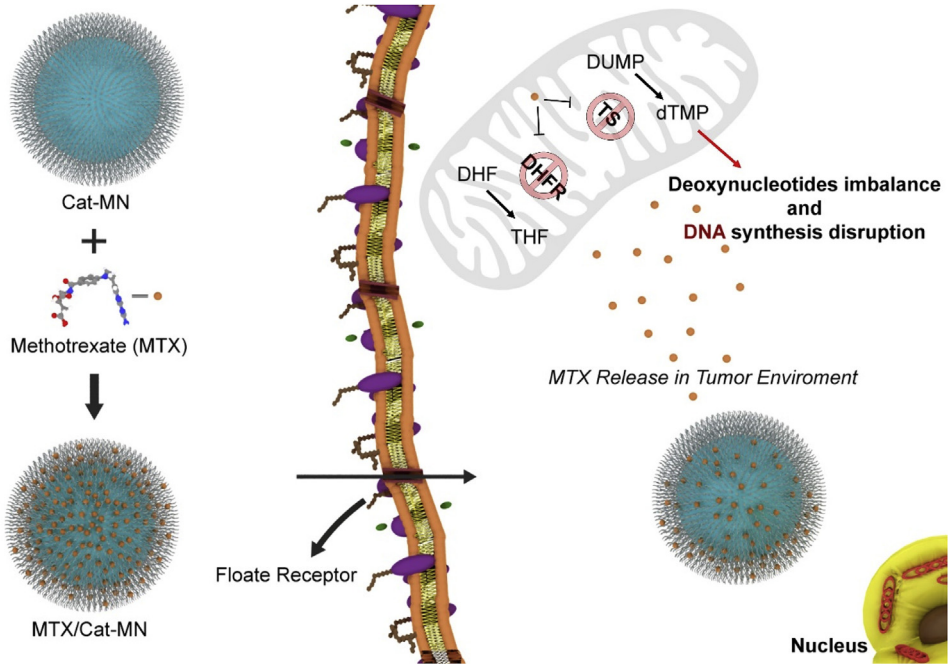

Fig. 10. MTX/Cat-MN internalization mechanism into the cancer cells via folate receptor channel and its drug release in acidic condition (dihydrofolate reductase = DHFR, dihydrofolate = DHF, THF = tetrahydrofolate, thymidylate synthase = TS, deoxyuridine monophosphate = dUMP, and deoxythymidine monophosphate = dTMP).

the results showed that Cat-MN has no substantial cytotoxic effects on cells and human red blood cells. MTT assay results have shown that the MTX/Cat-MN has more cytotoxicity on Saos-2 cells in comparison to MTX free form. Additionally, the successful cell internalization of the MTX/Cat-MN was qualitatively and quantitatively validated by the use of cellular uptake studies. All results persuaded us to suggest this biocompatible nano-system for therapeutic biomedical applications.

Funding

The research grant was provided by Drug Applied Research Center of Tabriz University of Medical Sciences for providing laboratory kits and staff costs (grant no: 58709).

Ethical approval number

IR.TBZMED.VCR.REC.1397.008.

CRediT authorship contribution statement

Delshad Ahmadi: Investigation. **Mojtaba Zarei:** Formal analysis. **Mahdi Rahimi:** Investigation. **Marzieh Khazaie:** Investigation. **Zatollah Asemi:** Writing - review & editing. **Seyed Mostafa Mir:** Investigation. **Alireza Sadeghpour:** Conceptualization. **Ansar Karimian:** Investigation. **Fourogh Alemi:** Investigation. **Mohammad Rahmati-Yamchi:** Investigation. **Roya Salehi:** Investigation. **Farhad Jadidi-Niaragh:** Investigation. **Mehdi Yousefi:** Investigation. **Nafiseh Khelgati:** Investigation. **Maryam Majidinia:** Conceptualization, Investigation. **Amin Safa:** Conceptualization, Writing - redf& editing. **Bahman Yousefi:** Conceptualization, Supervision, Writing -review & editing.

Declaration of competing interest

The authors report no conflicts of interest.

Acknowledgment

The Authors would like to thanks Clinical Research Development unit, Shohada hospital, Tabriz university of Medical Scinces, for kind supports.

Appendix A. Supplementary data

Supplementary data to this article can be found online at https://doi.org/10.1016/j.jddst.2020.101584.

References

[1] A.A. Endicott, et al., Perinatal factors associated with clinical presentation of osteosarcoma in children and adolescents, Pediatr. Blood Canc. 64 (6) (2017) e26349.
[2] F.R. Evola, M.E. Cucuzza, G. Evola, Osteosarcoma in the pediatric age, Euro-Mediterranean. Biomed. J. 13 (29) (2018) 127–131.
[3] R.L. Geary, et al., Osteosarcoma and second malignant neoplasms: a case series, Ir. J. Med. Sci. 188 (4) (2019) 1163–1167.
[4] B. Yousefi, et al., Akt and p53R2, partners that dictate the progression and invasiveness of cancer, DNA Repair 22 (9) (2014) 24–29.
[5] L. Wang, et al., The effective combination therapy against human osteosarcoma: doxorubicin plus curcumin co-encapsulated lipid-coated polymeric nanoparticulate drug delivery system, Drug Deliv. 23 (9) (2016) 3200–3208.
[6] M.W. Bishop, K.A. Janeway, R. Gorlick, Future directions in the treatment of osteosarcoma, Curr. Opin. Pediatr. 28 (1) (2016) 26–33.
[7] M. Hassanshahi, et al., Methotrexate chemotherapy–induced damages in bone marrow sinusoids: an in vivo and in vitro study, J. Cell. Biochem. 120 (3) (2019) 3220–3231.
[8] B. Yousefi, et al., Differential effects of peroxisome proliferator-activated receptor agonists on doxorubicin-resistant human myelogenous leukemia (k562/dox) cells, Cell. Mol. Biol. 61 (8) (2015) 118–122.
[9] Y. Shao, et al., Methotrexate induces astrocyte apoptosis by disrupting folate metabolism in the mouse juvenile central nervous system, Toxicol. Lett. 301 (2019) 146–156.
[10] D. Sandoval, G.S. Alarcón, Methotrexate, Atlas of Rheumatoid Arthritis, Springer, 2015, pp. 177–194.
[11] B. Friedman, B. Cronstein, Methotrexate mechanism in treatment of rheumatoid arthritis, Joint Bone Spine 86 (3) (2019) 301–307.
[12] K. Nejati-Koshki, et al., Synthesis and in vitro study of cisplatin-loaded Fe3O4 nanoparticles modified with PLGA-PEG6000 copolymers in treatment of lung cancer. J Microencapsul 31 (8) (2014) 815–823.
[13] F. ud Din, et al., Effective use of nanocarriers as drug delivery systems for the treatment of selected tumors, Int. J. Nanomed. 12 (2017) 7291.
[14] M. Rahimi, et al., Biocompatible magnetic tris(2-aminoethyl)amine functionalized nanocrystalline cellulose as a novel nanocarrier for anticancer drug delivery of methotrexate, New J. Chem. 41 (5) (2017) 2160–2168.
[15] S. Hossen, et al., Smart nanocarrier-based drug delivery systems for cancer therapy and toxicity studies: a review, J. Adv. Res. 15 (2019) 1–18.
[16] J.K. Patra, et al., Nano based drug delivery systems: recent developments and future prospects, J. Nanobiotechnol. 16 (1) (2018) 71.
[17] M. Rahimi, et al., Multi-branched ionic liquid-chitosan as a smart and biocompatible nano-vehicle for combination chemotherapy with stealth and targeted properties, Carbohydr. Polym. 196 (2018) 299–312.
[18] T.O.B. Olusanya, et al., Liposomal drug delivery systems and anticancer drugs, Molecules 23 (4) (2018) 907.

[19] V. Shafiei-Irannejad, et al., Reversion of multidrug resistance by co-encapsulation of doxorubicin and metformin in poly (lactide-co-glycolide)-d-α-tocopheryl polyethylene glycol 1000 succinate nanoparticles, Pharm. Res. (N. Y.) 35 (6) (2018) 119.
[20] M. Rahimi, et al., Needle-shaped amphoteric calix [4] arene as a magnetic nanocarrier for simultaneous delivery of anticancer drugs to the breast cancer cells, Int. J. Nanomed. 14 (2019) 2619.
[21] J.B. Miller, et al., Development of cationic quaternary ammonium sulfonamide amino lipids for nucleic acid delivery, ACS Appl. Mater. Interfaces 10 (3) (2018) 2302–2311.
[22] V. Shafiei-Irannejad, et al., Metformin enhances doxorubicin sensitivity via inhibition of doxorubicin efflux in P-gp-overexpressing MCF-7 cells, Chem. Biol. Drug Des. 91 (1) (2018) 269–276.
[23] M. Farshbaf, et al., pH-and thermo-sensitive MTX-loaded magnetic nanocomposites: synthesis, characterization, and in vitro studies on A549 lung cancer cell and MR imaging, Drug Dev. Ind. Pharm. 44 (3) (2018) 452–462.
[24] J.A. Faiz, N. Spencer, Z. Pikramenou, Acetylenic cyclodextrins for multireceptor architectures: cups with sticky ends for the formation of extension wires and junctions, Org. Biomol. Chem. 3 (23) (2005) 4239–4245.
[25] T.J. Malefetse, et al., Cyclodextrin-ionic liquid polyurethanes for application in drinking water treatment, Water Sa 35 (5) (2009).
[26] M. Rahimi, et al., Dendritic chitosan as a magnetic and biocompatible nanocarrier for the simultaneous delivery of doxorubicin and methotrexate to MCF-7 cell line, New J. Chem. 41 (8) (2017) 3177–3189.
[27] E. BahojbNoruzi, et al., Design of a thiosemicarbazide functionalized calix [4] arene ligand and related transition metal complexes: synthesis, characterization and biological studies, Front. Chem. 7 (2019) 663.